Hole Distribution in Underdoped and Overdoped $Y(Ba_{2-y}Sr_y)Cu_3O_{6+\delta}$ Compounds Studied by X-ray Absorption Spectroscopy

R. S. Liu,*,† C. Y. Chang,† and J. M. Chen‡

Department of Chemistry, National Taiwan University, Taipei, Taiwan, R.O.C., and Synchrotron Radiation Research Center (SRRC), Hsinchu, Taiwan, R.O.C

Received April 13, 1998

The hole distribution of underdoped and overdoped states in the $Y(Ba_{2-y}Sr_y)Cu_3O_{6+\delta}$ ($\delta \sim 0.1$ and 0.9) compounds has been observed by high-resolution O K-edge X-ray-absorption near-edge-structure spectra. The chemical substitution of Sr for Ba in the fully oxygenated $Y(Ba_{2-y}Sr_y)Cu_3O_{6+\delta}$ ($\delta \sim 0.9$) compounds gives rise to high hole concentrations within both the CuO_2 planes and the out-of-plane sites, leading to the overdoped state and the decrease in the superconducting transition temperature from 92 K for $y = 0$ to 84 K for $y = 0.8$. In contrast, an increase in the Sr content in the oxygen-deficient $Y(Ba_{2-y}Sr_y)Cu_3O_{6+\delta}$ ($\delta \sim 0.1$) compounds did not indicate superconductivity. The oxygen-deficient compounds exhibit underdoped state due to the low hole concentration.

Introduction

Isovalent chemical substitution of Sr^{2+} for Ba^{2+} in the high-T_c superconducting $Y(Ba_{2-y}Sr_y)Cu_3O_{6+\delta}$ ($\delta = 0.7-0.9$) system reduces the T_c value.[1−12] In contrast, replacement of Y^{3+} by various 3+ rare-earth ions (except Pr) has only minor effects on T_c. The series of $Y(Ba_{2-y}Sr_y)Cu_3O_{7-\delta}$ ($\delta = 0.7-0.9$) compounds have been studied by means of X-ray diffraction,[1,8−10,12] neutron diffraction,[6,11] extended X-ray-absorption fine structure (EXAFS),[4] X-ray absorption near-edge structure (XANES),[12] infrared spectra, and Raman scattering.[7,11] However, the reasons for the suppression of superconductivity in $Y(Ba_{2-y}Sr_y)Cu_3O_{6+\delta}$ have been a remarkable puzzle in the cuprate superconductors.

A local perturbation of the crystal structure in the neighborhood of the Sr sites (the oxygen vacancies along the CuO chains were induced by Sr doping) are well recognized as the possible model for explaining the depression of superconductivity in $Y(Ba_{2-y}Sr_y)Cu_3O_{6+\delta}$ ($\delta = 0.9$).[2] However, Ganguli and Subramanian[9] found the decrease in T_c in both series of $Y(Ba_{2-y}Sr_y)Cu_3O_{6+\delta}$ ($\delta = 0.7$ and 1) with fixed oxygen contents. Their results indicate that the oxygen vacancies cannot be the cause of the fall in T_c with Sr substitution. They also pointed out that the Sr substitution conducts about a similar decrease in T_c in the $Tl_2Ba_2CuO_6$ ($T_c = 90$ K) high-T_c superconductor.[14] Therefore, it should have some other reasons to control the depression of the T_c's in the $Y(Ba_{2-y}Sr_y)Cu_3O_{6+\delta}$ system.

It is well-known that hole states play a pivotal role in the p-type cuprate superconductors. Therefore, a knowledge of the electronic structure near the Fermi level of these compounds is an important step toward unveiling the mechanism of superconductivity. The X-ray absorption spectra are determined by electronic transitions from a selected atomic core level to the unoccupied electronic states near the Fermi level. X-ray absorption near edge structure is therefore a direct probe of the character and local density of hole states responsible for high-T_c superconductivity.

To improve the understanding on the mechanism of T_c suppression, a detailed study by using the X-ray absorption spectroscopy on $Y(Ba_{2-y}Sr_y)Cu_3O_{6+\delta}$ systems would be helpful. We therefore measure systematically the variations of electronic structure near the Fermi level for a series of $Y(Ba_{2-y}Sr_y)Cu_3O_{7-\delta}$ ($\delta = 0.1$ and 0.9) compounds by the XANES method. Although, Song *et al.*[12] have demonstrated the similar studies on the fully oxygenated $Y(Ba_{2-y}Sr_y)Cu_3O_{6+\delta}$ ($\delta = 0.9$) samples, they failed to observe the significant variation of the hole concentration as a function of the Sr doping. Moreover, to observe the intrinsic doping effect of Sr (rule out the contribution from the CuO chain sites), we also prepared the series of oxygen-deficient $Y(Ba_{2-y}Sr_y)Cu_3O_{6+\delta}$ ($\delta = 0.1$) compounds. In this study, a bulk- sensitive O K-edge X-ray fluorescence yield measurements in $Y(Ba_{2-y}Sr_y)Cu_3O_{7-\delta}$ for $\delta = 0.1$ and 0.9 were performed in order to investigate how the variation of hole states near the Fermi level induced by the Sr doping related to the superconductivity.

Experimental Section

The samples of $Y(Ba_{2-y}Sry)Cu_3O_{6+\delta}$ were prepared by mixing powders of Y_2O_3, $BaCO_3$, $SrCO_3$, and CuO. The mixtures were calcined at 950 °C for 20 h in air. The resulting mixtures were ground

† National Taiwan University.
‡ Synchrotron Radiation Research Center.

(1) Wada, T.; Adachi, S.; Mihara T.; Inaba, R. *Jpn. J. Appl. Phys.* **1987**, *26*, L706.
(2) Veal, B. W.; Kwok, W. K.; Umezawa, A.; Crabtree, G. W.; Jorgensen J. D.; Downey J. W.; Nowicki, L. J.; Mitchell, A. W.; Paulikas, A. P.; Sowers, C. H. *Appl. Phys. Lett.* **1987**, *51*, 279.
(3) Sung, H. M.; Kung, J. H.; Liang, J. M.; Liu, R. S.; Chen, Y. C.; Wu, P. T.; Chen, L. J. *Phycica C* **1988**, *153−155*, 866.
(4) Zhang, K.; Bunker, G.; Chance, B.; Gallo, C. F. *Phys. Rev. B* **1989**, *39*, 2788.
(5) Fueki, K.; Idemoto, Y.; Ishizuka, H. *Physica C* **1990**, *166*, 261.
(6) Strom, C.; Kall, M.; Jonannson, L. G.; Erilsson, S. G.; Borjesson, L. *Physica C* **1991**, *185*, 623.
(7) Yamamoto, H.; Mori, T.; Onari, S.; Arai, T. *Physica C* **1991**, *181*, 133.
(8) Karen, P.; Fjellvag, H.; Kjekshus, A.; Andresen, A. F. *J. Solid State Chem.* **1991**, *92*, 57.
(9) Ganguli, A. K.; Subramanian, M. A. *Mater. Res. Bull.* **1991**, *26*, 869.
(10) Golben, J.; Vlasse, M. *Supercond. Sci. Technol.* **1992**, *5*, 231.
(11) Kakihana, M.; Eriksson, S.-G., Borjesson, L.; Johansson, L.-G.; Strom, C.; Kall, M. *Phys. Rev. B* **1993**, *47*, 5359.
(12) Song, Y. F.; Lee, S. B.; Chang, C. N.; Liu, H. F.; Hsieh, C. H.; Horng, H. E. *Solid State Commun.* **1996**, *99*, 901.
(13) Lin, J. G.; Huang, C. Y.; Xue, Y. Y.; Chu, C. W.; Cao, X. W.; Ho, J. C. *Phys. Rev. B* **1995**, *51*, 12900.
(14) Ganguli, A. K.; Subramanian, M. A. *J. Solid State Chem.* **1991**, *90*, 382.

10.1021/ic980418m CCC: $15.00
Published on Web 09/30/1998

Table 1. Oxygen Contents of the Fully Oxygenated and Oxygen-Deficient $Y(Ba_{2-y}Sr_y)Cu_3O_{6+\delta}$ Samples

fully oxygenated		oxygen-deficient	
y	$6+\delta$	y	$6+\delta$
0	6.885 ± 0.018	0	6.10 ± 0.02
0.2	6.940 ± 0.005	0.2	6.10 ± 0.03
0.4	6.925 ± 0.005	0.4	6.13 ± 0.01
0.6	6.919 ± 0.006	0.8	6.12 ± 0.02
0.8	6.922 ± 0.015	1.0	6.20 ± 0.03

and pressed into pellets. The pellets were sintered at 950 °C for 20 h in air. The $\delta \sim 0.9$ (fully oxygenated) samples were obtained when the sintered pellets were annealed at 400 °C for 20 h in O_2. Moreover, the $\delta = 0.1$ (oxygen-deficient) samples were achieved by annealing the sintered pellets at 730 °C for 20 h in Ar then quenching into liquid nitrogen within 1 s.

X-ray powder diffraction measurements were carried out with a SCINTAG (X1) diffractometer (Cu Kα radiation). Data for the Rietveld refinement were collected in the 2θ range 20−110° with a step size of 0.02° and a count time of 10 s per step. The program of GSAS[15] was used for the Rietveld refinement in order to obtain the information of crystal structure of $Y(Ba_{2-y}Sr_y)Cu_3O_{6+\delta}$. Two chemical titration methods, namely iodometric titration[17] and modified iodometric titration[18] were used to determine the oxygen contents (δ) in the fully oxygenated and oxygen-deficient samples, respectively. In Table 1, we show the analytical results. The oxygen contents in the fully oxygenated and oxygen-deficient samples are determined to be around 0.92 and 0.13, respectively. Magnetization data were taken from a superconducting quantum interference device (SQUID) magnetometer (Quantum Design).

Using the 6-m high-energy spherical grating monochromator (HSGM) beamline, the X-ray absorption measurements were performed at the Synchrotron Radiation Research Center (SRRC) with an electron beam energy of 1.5 GeV and a maximum stored current of 240 mA. X-ray fluorescence-yield spectra were recorded using a microchannel plate (MCP) detector.[19] This MCP detector is composed of a dual set of MCPs with an electrically isolated grid mounted in front of them. X-ray fluorescence yield measurement is strictly bulk sensitive with a probing depth of around thousand angstroms. During the X-ray fluorescence yield measurements, the grid was set to a voltage of 100 V while the front of the MCPs was set to −2000 V and the rear to −200 V. The negative MCP bias was applied to expel electrons before they entered the detector, while the grid bias ensured that no positive ions were detected. The MCP detector was located at ∼2 cm from the sample and oriented parallel to the sample surface. Photons were incident at an angle of 45° with respect to the sample normal. The incident photon intensity (I_o) was measured simultaneously by a Ni mesh located after the exit slit of the monochromator. All the absorption spectra were normalized to I_o. The photon energy was calibrated using the known O K-edge absorption peaks of CuO. The energy resolution of the monochromator was set to ∼0.22 eV for the O K-edge X-ray absorption measurements. All the measurements were performed at room temperature.

Results and Discussion

The series of XRD spectra of the fully oxygenated ($\delta = 0.92$) $Y(Ba_{2-y}Sr_y)Cu_3O_{6+\delta}$ samples are shown in Figure 1. All the fully oxygenated samples are single phase with an orthorhombic crystal structure and can be indexed in the *Pmmm* space group. In Figure 2, we show the cell volume as a function of y in the fully oxygenated ($\delta = 0.92$) $Y(Ba_{2-y}Sr_y)Cu_3O_{6+\delta}$ series. The decrease in the cell volume with increasing the Sr content (y) was observed in fully oxygenated $Y(Ba_{2-y}Sr_y)Cu_3O_{6+\delta}$ ($\delta = 0.92$) samples. Moreover, the decrease in the lattice constants of a, b, and c with increasing y in the corresponding series samples has also been found (as shown in Figure 3). These are simply due to a manifestation of the smaller size of the substituting Sr^{2+} ion [1.36 Å for CN (coordination number) = 10] as compared to the bigger Ba^{2+} ions (1.52 Å for CN = 10).[16] The XRD patterns of the oxygen-deficient ($\delta = 0.13$) $Y(Ba_{2-y}Sr_y)Cu_3O_{6+\delta}$ samples as shown in Figure 4. The series samples are single phase with tetragonal crystal structure and can be indexed on the *P*4/*mmm* space group. In Figures 5 and 6, we show composition (y) dependence of cell volume and lattice constants (a and c) of the oxygen-deficient samples, respectively. Both of them are decreased as increasing x which are caused by the size effect.

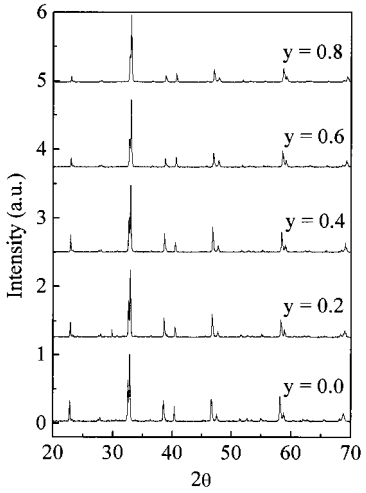

Figure 1. XRD spectra of the fully oxygenated ($\delta = 0.92$) $Y(Ba_{2-y}Sr_y)Cu_3O_{6+\delta}$ samples.

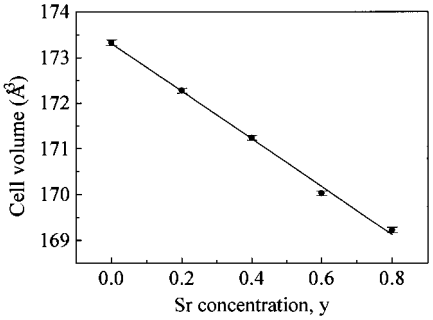

Figure 2. Cell volume as a function of y in the fully oxygenated ($\delta = 0.92$) $Y(Ba_{2-y}Sr_y)Cu_3O_{6+\delta}$ series.

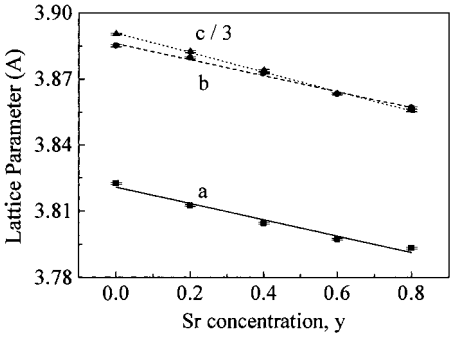

Figure 3. Lattice constants of a, b, and c as a function of y in the fully oxygenated ($\delta = 0.92$) $Y(Ba_{2-y}Sr_y)Cu_3O_{6+\delta}$ series.

(15) Larson, A. C.; Von Dreele, R. B. *Generalized Structure Analysis System*; Los Alamos National Laboratory: Los Alamos, NM, 1994.
(16) Shannon, R. D. *Acta Crystallogr. Sect. A* **1976**, *32*, 751.
(17) Appleman, E. H.; Morss, L. R.; Kini, A. M.; Geiser, U.; Umezawa, A.; Crabtree, G. W.; Carlson, K. D. *Inorg. Chem.* **1987**, *26*, 3237.
(18) Nazzal, A. I.; Lee V. Y.; Engler, E. M.; Jacowitz, R. D.; Tokura, Y.; Torrance, J. B. *Physica C* **1988**, *153*−*155*, 1367.
(19) Chen, J. M.; Chung, S. C.; Liu, R. S. *Solid State Commun.* **1996**, *99*, 493.

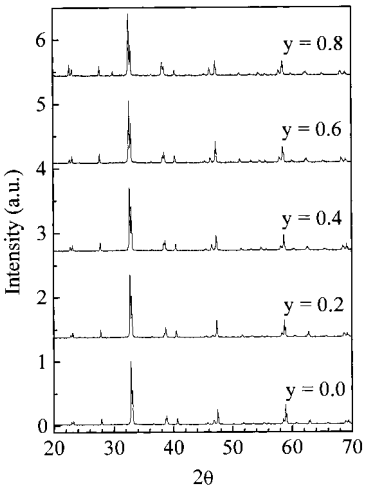

Figure 4. XRD patterns of the oxygen-deficient $Y(Ba_{2-y}Sr_y)Cu_3O_{6+\delta}$ ($\delta = 0.13$) samples.

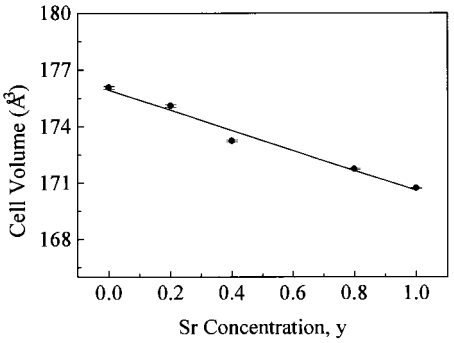

Figure 5. Composition (y) dependence of cell volume of the oxygen-deficient $Y(Ba_{2-y}Sr_y)Cu_3O_{6+\delta}$ ($\delta = 0.13$) samples.

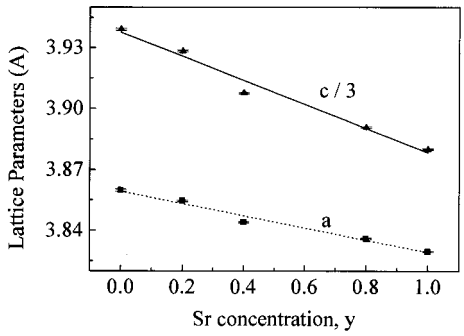

Figure 6. Lattice constants of a and c as a function of y in the oxygen-deficient $Y(Ba_{2-y}Sr_y)Cu_3O_{6+\delta}$ ($\delta = 0.13$) series.

The temperature dependence of low-field magnetization (10 G, field cooled) of the fully oxygenated $Y(Ba_{2-y}Sr_y)Cu_3O_{6+\delta}$ ($\delta = 0.92$) samples is shown in Figure 7. The derived value of T_c from Figure 7 as function of y in the fully oxygenated samples is shown in Figure 8. The isovalent chemical substitution of the Sr^{2+} ions for the Ba^{2+} ions in the corresponding series compounds leads to a monotonical decrease of the superconducting temperature from $T_c \sim 92$ K for $y = 0$ to $T_c \sim 84$ K for $y = 0.8$. In Figure 9, we show the temperature dependence of low field magnetization (10 G, field cooled) of the oxygen-deficient $Y(Ba_{2-y}Sr_y)Cu_3O_{6+\delta}$ ($\delta \sim 0.13$). An increase in the Sr content in the oxygen-deficient samples did not indicate superconductivity as shown in Figure 9.

It has been shown that core−hole effect in O 1s absorption spectrum can be ignored due to the strong similarity of O 1s absorption spectra and resonant high-energy inverse photoemission spectra on high-T_c $Bi_2Sr_2CaCu_2O_8$ cuprate.[20] On the basis of the dipole selection rules, only the local unoccupied states with the O 2p character, including both mobile and localized holes, are probed in the oxygen K-edge X-ray absorption spectra. Therefore, if the hole states near the Fermi level in the p-type cuprates are of primarily O 2p character, a preedge peak should be visible in the O 1s XANES spectrum with an intensity proportional to the O 2p hole concentration.

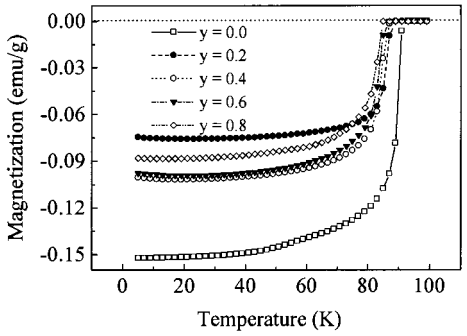

Figure 7. Temperature dependence of low-field magnetization (10 G, field cooled) of the fully oxygenated $Y(Ba_{2-y}Sr_y)Cu_3O_{6+\delta}$ ($\delta = 0.92$) samples.

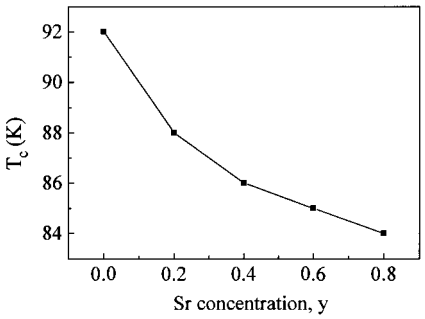

Figure 8. The T_c's as a function of y in the fully oxygenated ($\delta = 0.92$) $Y(Ba_{2-y}Sr_y)Cu_3O_{6+\delta}$ samples.

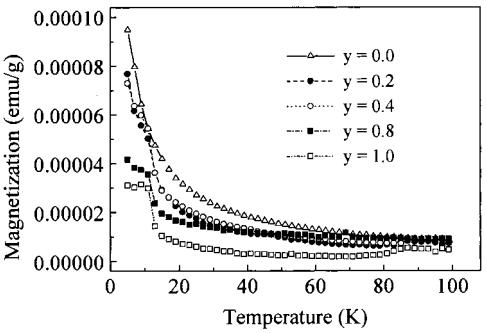

Figure 9. Temperature dependence of low field magnetization (10 G, field cooled) of the oxygen-deficient $Y(Ba_{2-y}Sr_y)Cu_3O_{6+\delta}$ ($\delta \sim 0.13$) samples.

In Figure 10, the O K-edge X-ray absorption spectra for a series of fully oxygenated $Y(Ba_{2-y}Sr_y)Cu_3O_{6+\delta}$ ($\delta \sim 0.92$) samples with $y = 0-0.8$ are shown in the energy range of 525−550 eV obtained using a bulk-sensitive total X-ray fluorescence yield technique. The major features in the O 1s X-ray absorption spectrum of the sample with $y = 0.4$, as shown in Figure 10, are three distinct prepeaks at ∼528.3, ∼529.3, and ∼530.5 eV, respectively, together with a shoulder at ∼527.7 eV and a broad peak at 537 eV. The low-energy prepeaks with energy below 532 eV are ascribed to photoexcitation of the O

(20) Wruke, W.; Himpsel, F. J.; Chandrashekar, G. V.; Shafer, M. W. *Phys. Rev. B* **1989**, *39*, 7328.

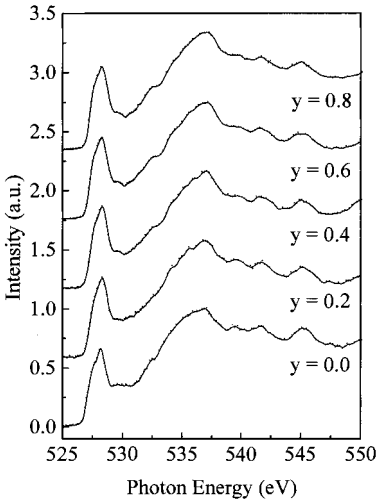

Figure 10. The O K-edge X-ray absorption spectra for a series of the fully oxygenated $Y(Ba_{2-y}Sr_y)Cu_3O_{6+\delta}$ ($\delta \sim 0.9$) samples with $y = 0-0.8$.

1s core electrons to holes with predominantly 2p character on the oxygen sites. Unoccupied states related to the Ba 4d and Y 5d states hybridized with O 2p states could be the origin for the enhanced peaks above 532 eV in $Y(Ba_{2-y}Sr_y)Cu_3O_{6+\delta}$ ($\delta \sim 0.92$). The O K-edge X-ray absorption spectra for various compounds with different y values in Figure 10 were normalized to the same height at the main peak of ~537 eV.

The crystal structure of fully oxygenated $YBa_2Cu_3O_{6+\delta}$ ($\delta \sim 0.92$) is composed of two Cu(2)O(2)O(3) (the atomic notation of Jorgensen *et al.*[21] is used) layers separated by a Y plane. The unit of CuO_2 and Y planes are separated by a CuO_3 ribbon consisting of a BaO(4) plane, a Cu(1)O(1) chain along the *b* axis, and another BaO(4) plane. Therefore, there exists four nonequivalent oxygen sites: O(2) and O(3) within the Cu(2)-O_2 layers, O(4) in the BaO planes, and O(1) in the Cu(1)O(1) chains. With respect to the O 1s edge, the observed different O 1s thresholds in Figure 10 may be a result of chemical shifts due to the influence of charges on the oxygen sites and the site-specific neighborhood. Band-structure calculations based on the local-density approximation (LDA) have been successful to calculate the electronic structure of the cuprate superconductors.[22] According to the LDA band-structure calculations in $YBa_2Cu_3O_{6+\delta}$ ($\delta = 0.9-1$) by Krakauer et al.,[23] the O(2,3) atoms in the CuO_2 planes and the O(1) atom in the CuO chain are predicted to have the largest and the lowest binding energy of the O 1s level, respectively. Moreover, based on the polarization-dependent X-ray absorption measurements on a single crystal of $YBa_2Cu_3O_{6+\delta}$ ($\delta = 0.9-1$), it was found that O(2) 1s level is about 0.8 eV lower in energy than the O(4) 1s level.[24] The O(1) 1s binding energy is between those of O(4) and O(2,3). These results are consistent with the theoretical prediction. In O K-edge X-ray absorption spectra of $YBa_2Cu_3O_{6+\delta}$ ($\delta = 0.9-1$), the prepeaks at ~527.8 eV are attributed to transitions into O 2p holes in the CuO_3 ribbons (apical oxygen sites and CuO chains). The high-energy prepeak at ~528.5 eV is ascribed to transitions into O 2p hole states within the CuO_2 planes.[24,25]

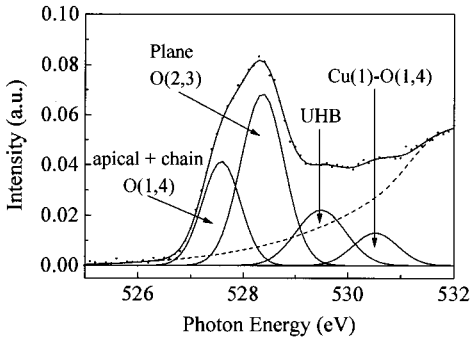

Figure 11. A typical curve fit of four Gaussians to the O 1s preedge peak of $Y(Ba_{2-y}Sr_y)Cu_3O_{6+\delta}$ ($\delta \sim 0.9$) with $y = 0.4$.

The orthorhombic $Y(Ba_{2-y}Sr_y)Cu_3O_{6+\delta}$ ($\delta \sim 0.92$) compounds are isomorphic with $YBa_2Cu_3O_{6+\delta}$ ($\delta = 0.9-1$) (space group: *Pmmm*). With the increase in the Sr content in $Y(Ba_{2-y}Sr_y)Cu_3O_{6+\delta}$ ($\delta \sim 0.92$), the compounds still keep the orthorhombic form. We did not observe any phase transition (from orthorhombic to tetragonal) at a particular Sr concentration in the $Y(Ba_{2-y}Sr_y)Cu_3O_{6+\delta}$ ($\delta \sim 0.92$; $y = 0-0.8$) system. As shown in Figure 10, the O 1s X-ray absorption spectrum of $Y(Ba_{2-y}Sr_y)Cu_3O_{6+\delta}$ ($\delta \sim 0.92$) with $y = 0.4$ exhibits similar features as observed in $YBa_2Cu_3O_{6+\delta}$ ($\delta = 0.9-1$). We therefore adopt the same assignment scheme for the O 1s X-ray absorption spectra of $Y(Ba_{2-y}Sr_y)Cu_3O_{6+\delta}$ ($\delta \sim 0.92$). The high-energy prepeak at ~528.3 eV is attributed to the excitation of O 1s electrons to O 2p holes in the CuO_2 planes. The low-energy prepeaks at ~527.7 eV in Figure 10 are due to the superposition of O 2p hole states in the apical oxygen sites [O(1) and the CuO(1) chains. The peaks at 527.7 and 528.3 eV correspond to the transitions from O 1s state into the valence band.

The peak at about 529.3 eV is ascribed to transitions into the conduction band (upper Hubbard band) which is predominantly formed by the hybridization in the ground state of the $Cu3d^9$ and $Cu3d^{10}L$ states, where L is ligand hole from the O 2p band.[24,25] Due to the strong on-site correlation effects on the copper sites in the cuprate superconductors, upper Hubbard band (UHB) has always been assumed to exist. Moreover, the peak at ~530.5 eV (as shown in Figure 10) is due to the transition into the mixing state between $Cu(1)3d_{y^2-z^2}$ and O(1,4)-$2p_{y,z}$.[24]

To investigate the variation of the hole states among different oxygen sites as a function of the Sr doping, these preedge features shown in Figure 10 were analyzed by fitting Gaussian functions to each spectrum. In Figure 11 we show a typical curve fitting of four Gaussians to the O 1s preedge peak of $Y(Ba_{2-y}Sr_y)Cu_3O_{6+\delta}$ ($\delta \sim 0.92$) with $y = 0.4$.

In Figure 12 the integrated intensity of each prepeak, normalized against that of main peak at ~537 eV, is plotted as a function of Sr content y in $Y(Ba_{2-y}Sr_y)Cu_3O_{6+\delta}$ ($\delta \sim 0.92$). As noted from Figure 12, the hole contents from the CuO_2 planes and apical and chain sites increase with increasing the Sr doping for $y < 0.6$ and saturate for $y > 0.6$. This clearly reveals that the overdoped state among the plane, apical and chain oxygen sites can be achieved by the Sr doping in the fully oxygenated $YBa_2Cu_3O_{6+\delta}$ ($\delta \sim 0.92$) sample. The higher the Sr doping will give rise to a heavier doping state and lead to the depression of T_c's in $Y(Ba_{2-y}Sr_y)Cu_3O_{6+\delta}$ ($\delta \sim 0.92$). It is also noted out that the intensity for the upper Habber bands is also increased as the Sr doping. This phenomenon is not clear at this stage.

(21) Jorgensen, J. D.; Veal, B. W.; Paulikas, A. P.; Nowicki, L. J.; Crabtree, G. W.; Claus, H.; Kwok, W. K. *Phys. Rev. B* **1990**, *41*, 1863.
(22) Emary, V. J. *Phys. Rev. Lett.* **1987**, *58*, 2794.
(23) Krakauer, H.; Pickett, W. E.; Cohen, R. E. *J. Supercond.* **1988**, *1*, 111.
(24) Nucker, N.; Pellegrin, E.; Schweiss, P.; Fink, J.; Molodtsov, S. L.; Simmons, C. T.; Kaindl, G.; Frentru, W.; Erb. A.; Muller-Vogt, G. *Phys. Rev. B* **1995**, *51*, 8529.
(25) Fink, J.; Nucker, N.; Pellegrin, E.; Romberg, H.; Alexander, M.; Knupfer, M. *J. Electron Spectrosc. Relat. Phenom.* **1994**, *66*, 395.

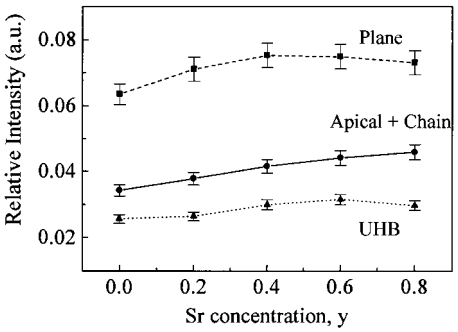

Figure 12. The integrated intensity of each prepeak, normalized against that of main peak at ~537 eV, is plotted as a function of Sr content y in $Y(Ba_{2-y}Sr_y)Cu_3O_{6+\delta}$ ($\delta \sim 0.9$).

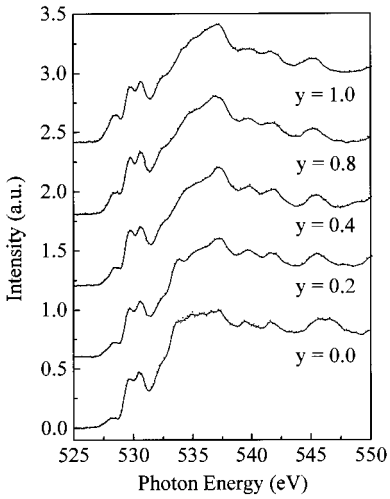

Figure 13. The O K-edge X-ray absorption spectra for a series of oxygen-deficient $Y(Ba_{2-y}Sr_y)Cu_3O_{6+\delta}$ ($\delta \sim 0.13$) samples with $y = 0-1.0$.

To get rid of the contribution from the Cu(1)O(4) chain, the intrinsic contribution of Sr doping in the oxygen-deficient $Y(Ba_{2-y}Sr_y)Cu_3O_{6+\delta}$ ($\delta \sim 0.1$) can fit the goal. In Figure 13, the O K-edge X-ray absorption spectra for a series of oxygen-deficient $Y(Ba_{2-y}Sr_y)Cu_3O_{6+\delta}$ ($\delta \sim 0.13$) samples with $y = 0-1.0$ are shown in the energy range of 525−550 eV obtained using a bulk-sensitive total X-ray fluorescence yield method. The major features in the O 1s X-ray absorption spectrum of such samples, as shown in Figure 13, are similar to those in Figure 10. We therefore apply the similar approach to analyze the variation of the hole states among different oxygen sites as a function of the Sr doping. In Figure 14 the integrated intensity of each prepeak, normalized against that of main peak at ~537 eV, is plotted as a function of Sr content y in $Y(Ba_{2-y}Sr_y)Cu_3O_{6+\delta}$

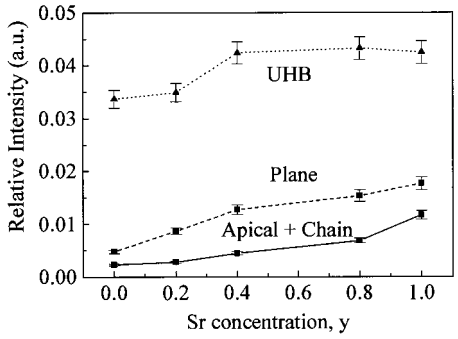

Figure 14. The integrated intensity of each prepeak, normalized against that of main peak at ~537 eV, is plotted as a function of Sr content y in $Y(Ba_{2-y}Sr_y)Cu_3O_{6+\delta}$ ($\delta \sim 0.13$).

($\delta \sim 0.13$). On the basis of the results as shown in Figure 14, we can conclude that the hole concentration within the plane, apical and chain oxygen sites can be increased as increasing the Sr content in the oxygen-deficient $Y(Ba_{2-y}Sr_y)Cu_3O_{6+\delta}$ ($\delta \sim 0.13$) samples. It again confirms that the Sr doping can effectively increase the hole concentration in the cuprate superconductors. However, the hole concentration within the oxygen-deficient $Y(Ba_{2-y}Sr_y)Cu_3O_{6+\delta}$ ($\delta \sim 0.13$) samples is still not enough to induce the superconductivity.

No matter what the Sr doping in the fully oxygenated $YBa_2Cu_3O_{6+\delta}$ ($\delta \sim 0.92$) or oxygen-deficient $Y(Ba_{2-y}Sr_y)Cu_3O_{6+\delta}$ ($\delta \sim 0.1$), the increase in the hole concentration of the cuprates has found which may be due to the contraction of the lattice constant as increasing Sr doping and give rise to better hybridization between Cu 3d and O 2p states. In this study, we reported the O 1s-edge X-ray absorption spectra for a series of $Y(Ba_{2-y}Sr_y)Cu_3O_{6+\delta}$ ($\delta \sim 0.1$ and 0.9) compounds. Near the O 1s edge, the multiple prepeaks is related to the different O 1s binding energies of the nonequivalent oxygen sites in the crystal structure. As deduced from the O 1s X-ray absorption spectra, the hole concentrations originating from the CuO_2 planes and CuO_3 ribbons can be increased in $Y(Ba_{2-y}Sr_y)Cu_3O_{6+\delta}$ ($\delta \sim 0.1$ and 0.9) with increasing the Sr doping. The present XANES results clearly demonstrate that the superconductivity suppression with the Sr substitution in fully oxygenated $Y(Ba_{2-y}Sr_y)Cu_3O_{6+\delta}$ ($\delta \sim 0.92$) arises predominantly from overdoping. However, absence superconductivity in oxygen-deficient $Y(Ba_{2-y}Sr_y)Cu_3O_{6+\delta}$ ($\delta \sim 0.13$) via Sr doping is due to low hole concentration in an underdoped state.

Acknowledgment. This research is financially supported by National Science Council of the Republic of China under Grant Number NSC 87-2113-M-002-005. We thank Dr. P. Nachimuthu for helping us revise the plots.

IC980418M